Effect of hydrostatic pressure on magnetic phase transition and magnetocaloric properties of $(Sm_{0.8}Nd_{0.2})_{0.52}Sr_{0.48}MnO_3$

S. Arumugam,[1,a)] P. Sarkar,[2,3,b)] P. Mandal,[3] A. Murugeswari,[1] K. Matsubayashi,[4] C. Ganguli,[4] and Y. Uwatoko[4]
[1]*Centre for High Pressure Research, School of Physics, Bharathidasan University, Tiruchirappalli 620 024, India*
[2]*Department of Physics, Serampore College, Serampore 712 201, India*
[3]*Saha Institute of Nuclear Physics, 1/AF Bidhannagar, Calcutta 700 064, India*
[4]*ISSP, University of Tokyo, 5-1-5 Kashiwanoha, Kashiwa, Chiba 277-8581, Japan*

(Received 10 April 2010; accepted 22 April 2010; published online 1 June 2010)

We have investigated the effect of hydrostatic pressure (P) on ferromagnetic (FM) phase transition and magnetocaloric properties of $(Sm_{0.8}Nd_{0.2})_{0.52}Sr_{0.48}MnO_3$ single crystal. At ambient pressure, the system undergoes a first order FM transition associated with large magnetic entropy change (ΔS_M). The temperature distribution of ΔS_M exhibits an asymmetric behavior with respect to T_C. The application of pressure increases magnetization, shifts the FM transition to higher temperature, and weakens the metamagnetism. As a result, $|\Delta S_M|$ decreases and its thermal distribution becomes more symmetric as compared to $P=0$. © *2010 American Institute of Physics*. [doi:10.1063/1.3431343]

I. INTRODUCTION

Perovskite manganites $R_{1-x}A_xMnO_3$ (R: rare-earth ions, A: alkaline-earth ions) have extensively been studied in the light of close interplay among spin, charge, and orbital degrees of freedom.[1–5] For $R_{1-x}A_xMnO_3$, one of the key parameters to determine the nature of the electronic or magnetic phase is the transfer interaction of e_g electrons or the effective band-width of e_g band. The bandwidth of a system can be controlled by tuning the average ionic radius r_0 of R and A cations $[r_0=(1-x)r_R+xr_A]$.[6] A decrease in r_0 leads to an increase in the tilting of MnO_6 octahedra, and hence a decrease in bandwidth. Thus, one can change the material properties dramatically through substitution. However, substitution itself introduces local strain due to the quenched disorder arising mainly from the size mismatch between R and A ions.[5,7] Several groups have studied the effect of quenched disorder on the nature of phase transition and found that narrowband manganites with large quenched disorder exhibit a first-order ferromagnetic (FM) to paramagnetic (PM) phase transition, whereas, broadband manganites with high Curie temperature (T_C) undergo conventional second-order transition.[4,5,7–11]

It has been observed that materials exhibiting first-order transition reveal significant amount of magnetic entropy change (ΔS_M), i.e., a large magnetocaloric effect (MCE).[12–15] Both the theoretical and experimental studies have revealed that the first-order character of the transition in disordered manganites can be changed by applying external perturbations like magnetic field (H) and hydrostatic pressure (P).[9–11,16–19] As ΔS_M is sensitive to the nature of magnetic phase transition, the MCE in narrowband manganites is expected to show strong dependence on external perturbations.

In this paper, we comprehensively describe the influence of hydrostatic pressure on the nature of FM–PM phase transition as well as magnetocaloric properties in $(Sm_{0.8}Nd_{0.2})_{0.52}Sr_{0.48}MnO_3$ single crystal. At ambient pressure, FM transition is first-order and the temperature profile of magnetic entropy is highly asymmetric. With the application of pressure, T_C increases, the first-order character of the transition gets suppressed, and the asymmetry in the entropy distribution reduces.

II. EXPERIMENTS

The single crystals of $(Sm_{0.8}Nd_{0.2})_{0.52}Sr_{0.48}MnO_3$ have been prepared by floating zone technique. The starting materials Sm_2O_3, Nd_2O_3, $SrCO_3$, and Mn_3O_4 were weighted to prescribed ratio and mixed by using ethanol. The mixture was calcined in air at ~1100 °C for 20 h and then pulverized. This procedure was repeated twice. The resultant powder was formed to cylindrical shape with use of hydrostatic pressure of ~5 ton to make a feed rod and sintered it again at ~1300 °C for 18 h to get a high density rod. The apparatus used for crystal growth was the floating zone image furnace equipped with two halogen incandescent lamps and hemielliptic focusing mirrors (NEC SC-M15 HD). The feed and seed rods were rotated in opposite directions for about 25 rpm. The molten zone was vertically scanned at a rate of 10 mm/h in oxygen atmosphere. The quality of the crystal was carefully checked by various techniques such as electron dispersive x-ray analysis, x-ray powder diffraction, Laue diffraction, ac susceptibility, etc. Another important measurement of crystal perfection in manganites is the ratio of the peak resistivity to the residual resistivity at low temperature, which is quite large in the studied crystal.[11] The magnetization measurements at ambient and 11.7 kbar pressures were performed by using a superconducting quantum interference device magnetometer (MPMS, Quantum Design) in fields up to 5 T. Magnetization under pressure was measured by using a self-clamp-type hybrid hydrostatic pressure cell, and the

a)Electronic mail: sarumugam1963@yahoo.com.
b)Electronic mail: babu2jit@yahoo.com.

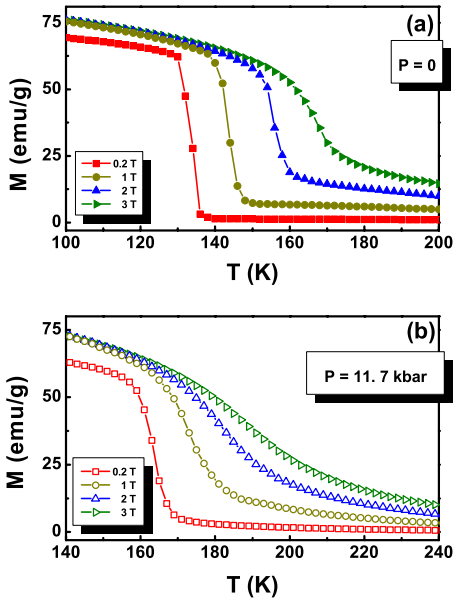

FIG. 1. (Color online) (a) Temperature dependence of magnetization (M) of $(Sm_{0.8}Nd_{0.2})_{0.52}Sr_{0.48}MnO_3$ single crystal for various magnetic fields (H) at ambient pressure ($P=0$). (b) $M(T)$ curves at $P=11.7$ kbar.

pressure was monitored using a manganin resistance device. The data were collected at 3 to 5 K interval after stabilizing the temperature for about 30 min. External magnetic field was applied along the longest sample direction to minimize the demagnetization effect.

III. RESULTS AND DISCUSSION

Figures 1(a) and 1(b) show the temperature dependence of magnetization (M) of $(Sm_{0.8}Nd_{0.2})_{0.52}Sr_{0.48}MnO_3$ single crystal for various magnetic fields at $P=0$ kbar and 11.7 kbar, respectively. For $P=0$, M shows a sharp FM transition at $T_C \approx 136$ K. The thermal hysteresis of M at $P=0$ is shown in the inset of Fig. 2. The presence of hysteresis has also been observed in resistivity and thermopower. With increasing H, T_C increases but the discontinuous nature of the $M(T)$ curve persists up to 2 T. These are general features of $M(T)$ curve of a system undergoing first-order FM transition. M increases and the transition shifts toward higher temperature ($T_C \approx 165$ K) with the application of pressure (11.7 kbar).

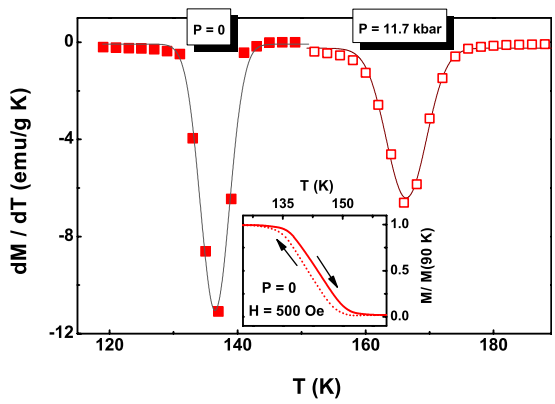

FIG. 2. (Color online) Temperature dependence of dM/dT for $P=0$ and 11.7 kbar at $H=0.2$ T. Inset shows the thermal hysteresis of M at $P=0$.

Also, the temperature variation in M for different fields becomes quite smooth at $P=11.7$ kbar. For qualitative analysis, we have calculated the temperature derivative (dM/dT) of magnetization for $P=0$ and 11.7 kbar. One can see that dM/dT versus T curve shows a sharp and narrow peak near the transition temperature for $P=0$, whereas the peak for $P=11.7$ kbar becomes broad in nature (Fig. 2). These results suggest that the first-order nature of the FM transition gets weakened in presence of external pressure.

In order to understand the pressure induced change in the nature of FM transition, we have also measured $M(H)$ isotherms both for $P=0$ and 11.7 kbar in the vicinity of T_C. Figure 3(a) displays the $M(H)$ isotherms for $P=0$. Below T_C, the data are typical of a ferromagnet. Initially, M increases rapidly with H and then reaches to saturation and its magnitude gradually decreases with increasing temperature. But above T_C, there is a significant change in the nature of $M(H)$ curve. M increases almost linearly up to a critical field followed by a steplike jump and reaches saturation. The value of critical magnetic field increases with increasing temperature. This behavior actually reflects a first order metamagnetic transition from PM to FM state. Earlier studies established that the field-induced metamagnetic transition in this system is due to the formation of inhomogeneous metastable state in the presence of quenched disorder.[7–9] The sharpness of the metamagnetic transition can be understood by taking into account the field dependence of differential susceptibility (dM/dH). The sharp peak in dM/dH versus H curve above T_C is the clear indication of first-order metamagnetic transition [inset of Fig. 3(b)]. For further verification about the order of transition, we have plotted H/M versus M^2 isotherms (Arrott plots)[20] in the vicinity of T_C for $P=0$ [Fig. 3(b)]. According to the Banerjee criterion, the slope of H/M versus M^2 plot should be negative for a first-order magnetic transition.[21] The large negative slope of H/M versus M^2 curve below $H \approx 2$ T confirms that the FM transition is first-order at ambient pressure. On the other hand, for $P=11.7$ kbar, the steplike jump in $M(H)$ has not been observed and the isotherms are more or less conventional FM type [Fig. 3(c)]. But the presence of peak in $dM(H)/dH$ curve [inset of Fig. 3(d)] indicates that the transition is still first-order metamagnetic because for a second-order transition, dM/dH should continuously decrease with H without showing any peak. However, the height of the peak in dM/dH is considerably reduced and the width is large as compared to that observed at ambient pressure. The broadening of the peak suggests that the first-order nature of the metamagnetic transition weakens with applied pressure. This can also be verified from the nature of Arrott plots for $P=11.7$ kbar [Fig. 3(d)]. With decreasing M^2, H/M decreases rapidly followed by a flat plateau-like feature over a wide range of M^2 and shows a marginal increase only in the low-field regime. This indicates that the FM–PM transition at $P=11.7$ kbar is in the verge of first-order and second-order transition.

Systems with sharp metamagnetic transition usually exhibit large MCE. The thermal variation in MCE in terms of

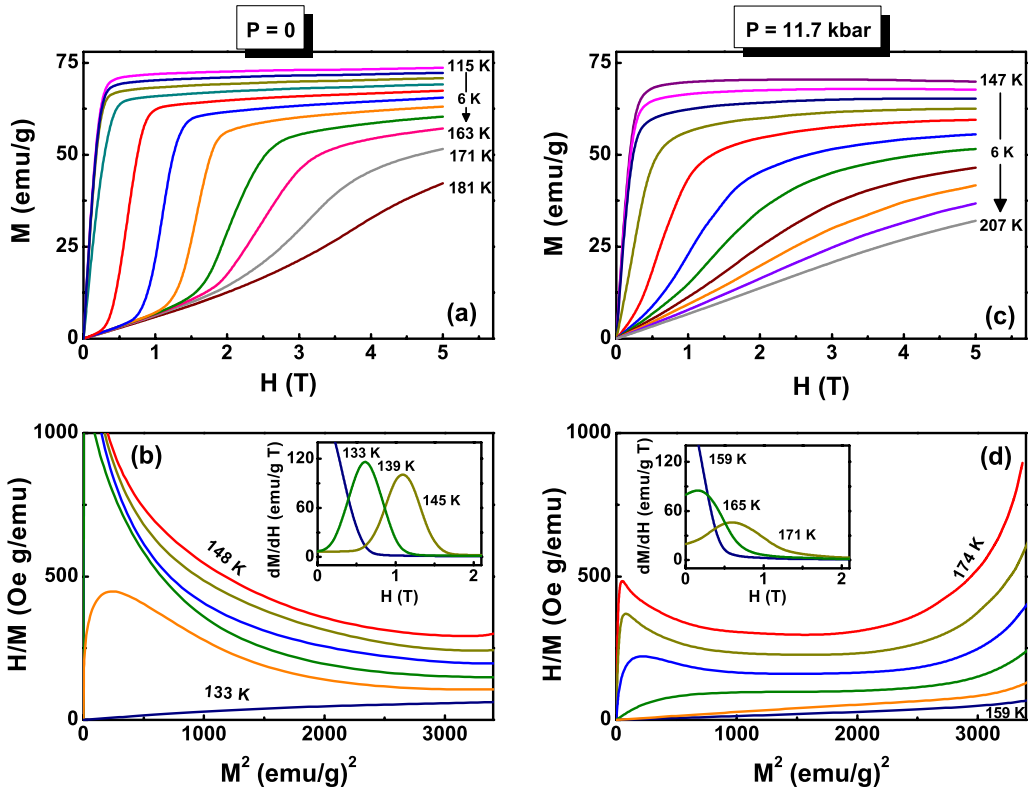

FIG. 3. (Color online) (a) Magnetization isotherms $[M(H)]$ of $(Sm_{0.8}Nd_{0.2})_{0.52}Sr_{0.48}MnO_3$ single crystal at $P=0$. (b) H/M vs M^2 plot of above $M(H)$ isotherms for 133 K$\leq T\leq$148 K in 3 K interval. Inset shows the H dependence of differential susceptibility (dM/dH) at ambient pressure. (c) $M(H)$ isotherms in the presence of $P=11.7$ kbar. (d) H/M vs M^2 plot of $M(H)$ isotherms at $P=11.7$ kbar for 159 K$\leq T\leq$174 K in 3 K interval. Inset shows the H dependence of dM/dH at $P=11.7$ kbar.

ΔS_M for $P=0$ kbar and 11.7 kbar is shown in Figs. 4(a) and 4(b), respectively. The values of ΔS_M have been calculated with the help of magnetization isotherms and employing the Maxwell relation[22]

$$\Delta S_M(T,H) = \int_0^H (\partial M/\partial T)_H dH. \quad (1)$$

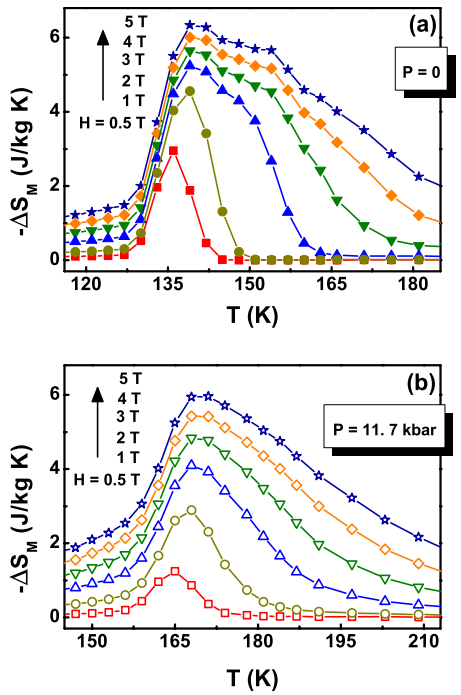

FIG. 4. (Color online) Temperature dependence of magnetic entropy change $(-\Delta S_M)$ of $(Sm_{0.8}Nd_{0.2})_{0.52}Sr_{0.48}MnO_3$ for different H for (a) at ambient pressure and (b) at $P=11.7$ kbar.

Equation (1) reveals that ΔS_M is proportional to $\partial M/\partial T$ at constant H. Therefore, it is expected that for a given H, ΔS_M attains its maximum value in the vicinity of T_C and decreases monotonically both below and above T_C. Beside this general behavior, there is a significant difference in the ΔS_M distribution between $P=0$ and 11.7 kbar. For $P=0$, ΔS_M increases rapidly with T, attains a maximum value around T_C and then decreases gradually, showing a large asymmetric behavior with respect to T_C in its thermal distribution. Such a typical nature of $\Delta S_M(T)$ has been observed in several FM systems showing first-order magnetic transition.[14,15] For a first-order transition, M shows a sharp drop at T_C at low magnetic fields. With increasing H, T_C increases and the transition becomes more gradual. Once a field larger than the critical magnetic field for the metamagnetic transition is applied, a plateau in ΔS_M is observed. Higher fields simply increase the width of the distribution but not the height as they cannot change entropy anymore. In contrary, the peak in $\Delta S_M(T)$ for $P=11.7$ kbar reduces in magnitude, shifts toward the higher temperature, and becomes less asymmetric as compared to $P=0$ case.

The maximum value of $-\Delta S_M(-\Delta S_M^{max})$ is plotted as a function of H in Fig. 5(a). For $P=0$, a faster increase in $-\Delta S_M^{max}(H)$ has been observed in the low-field regime, which is originating due to the field-induced first-order metamagnetic transition from PM to FM state. Further increase in H

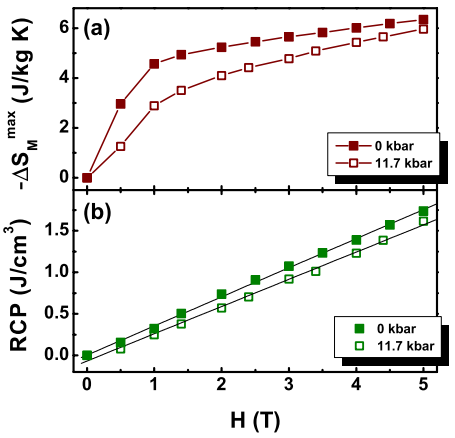

FIG. 5. (Color online) H dependence of (a) maximum value of magnetic entropy change ($-\Delta S_M^{max}$) and (b) RCP both at $P=0$ and 11.7 kbar.

enhances $-\Delta S_M$ at a slower rate. At $P=11.7$ kbar, the step-like behavior in $M(H)$ diminishes, FM transition becomes weakly first-order in nature and as a consequence almost continuous increase in $-\Delta S_M^{max}(H)$ is observed. Though the value of $-\Delta S_M^{max}$ at ambient pressure is higher as compared to that for $P=11.7$ kbar in the low-field region, the difference gradually decreases and disappears at high fields. With increasing P, the decrease as well as increase in $-\Delta S_M$ have been observed in many systems.[23] $-\Delta S_M$ decreases in nickel-rich Ni–Mn–Ga Heusler alloys while increases in $SmMn_2Ge_2$, $GdMn_2Ge_2$ and $MnAs_{0.93}Sb_{0.07}$ compounds.[23] Comparing the present value of $-\Delta S_M^{max}$ for $P=0$ with that for several reported magnetic refrigerants including manganites with T_C in the range of 50–150 K, we find that $(Sm_{0.8}Nd_{0.2})_{0.52}Sr_{0.48}MnO_3$ shows quite large ΔS_M particularly in the low-field region.[12,13,24] The magnetic refrigerant capacity or the relative cooling power (RCP), which is the measure of the amount of heat transfer between the hot and cold sinks during one ideal refrigeration cycle can be defined as[12,25]

$$\mathrm{RCP} = -\Delta S_M^{max} \times \delta T_{\mathrm{FWHM}}, \tag{2}$$

where δT_{FWHM} is the full-width at half-maximum of ΔS_M versus T plot. Using Eq. (2), RCP is calculated for different H. Both for $P=0$ and 11.7 kbar, RCP increases almost linearly with increasing H but the magnitude of RCP decreases with applied pressure [Fig. 5(b)].

It is thus clear that the magnetocaloric properties of this system are strongly correlated with the nature magnetic phase transition. At ambient pressure, the FM transition is first-order and the corresponding $\Delta S_M - T$ curves are asymmetric. With the application of pressure, Mn–O bond length decreases and Mn–O–Mn bond angle increases. As these changes enhance the effective charge transfer process, the band-width of the system increases and hence the FM metallic phase is stabilized. As a result, T_C increases, the first-order nature of the transition gets weakened, and the $\Delta S_M - T$ curves become more symmetric.

IV. CONCLUSIONS

We have studied the pressure dependent change in the nature of magnetic phase transition and magnetocaloric properties of $(Sm_{0.8}Nd_{0.2})_{0.52}Sr_{0.48}MnO_3$. For $P=0$, magnetization data show a first-order FM to PM phase transition, with a sharp change in M at T_C with thermal hysteresis and a large negative slope in H/M versus M^2 curves. The shape of T dependence of ΔS_M curve is asymmetric with respect to T_C. In contrast, for $P=11.7$ kbar, the transition becomes weakly first-order in nature and the ΔS_M distribution becomes more symmetric with the peak shifted toward the higher temperature side.

ACKNOWLEDGMENTS

The authors would like to thank Mr. A. Pal for technical assistance. One of us (S.A.) acknowledges the DST and UGC for their financial support.

[1] Y. Tokura and N. Nagaosa, Science **288**, 462 (2000).
[2] E. Dagotto, T. Hotta, and A. Moreo, Phys. Rep. **344**, 1 (2001).
[3] Y. Tokura, Rep. Prog. Phys. **69**, 797 (2006).
[4] H. Kuwahara, Y. Moritomo, Y. Tomioka, A. Asamitsu, M. Kasai, R. Kumai, and Y. Tokura, Phys. Rev. B **56**, 9386 (1997); Y. Tomioka, H. Kuwahara, A. Asamitsu, M. Kasai, and Y. Tokura, Appl. Phys. Lett. **70**, 3609 (1997).
[5] Y. Tomioka and Y. Tokura, Phys. Rev. B **70**, 014432 (2004).
[6] J. B. Torrance, P. Lacorre, A. I. Nazzal, E. J. Ansaldo, and C. Niedermayer, Phys. Rev. B **45**, 8209 (1992).
[7] L. M. Fisher, A. V. Kalinov, I. F. Voloshin, N. A. Babushkina, D. I. Khomshkii, Y. Zhang, and T. T. M. Palstra, Phys. Rev. B **70**, 212411 (2004).
[8] P. Sarkar and P. Mandal, Appl. Phys. Lett. **92**, 052501 (2008).
[9] P. Sarkar, P. Mandal, A. K. Bera, S. M. Yusuf, L. S. Sharath Chandra, and V. Ganesan, Phys. Rev. B **78**, 012415 (2008).
[10] L. Demkó, I. Kézsmárki, G. Mihály, N. Takeshita, Y. Tomioka, and Y. Tokura, Phys. Rev. Lett. **101**, 037206 (2008).
[11] P. Sarkar, P. Mandal, K. Mydeen, A. K. Bera, S. M. Yusuf, S. Arumugam, C. Q. Jin, T. Ishida, and S. Noguchi, Phys. Rev. B **79**, 144431 (2009).
[12] K. A. Gschneidner, Jr., V. K. Pecharsky, and A. O. Tsokol, Rep. Prog. Phys. **68**, 1479 (2005) and references herein.
[13] M. H. Phan and S. C. Yu, J. Magn. Magn. Mater. **308**, 325 (2007) and references herein.
[14] H. Wada and Y. Tanabe, Appl. Phys. Lett. **79**, 3302 (2001).
[15] V. K. Pecharsky, K. A. Gschneidner, Jr., A. O. Pecharsky, and A. M. Tishin, Phys. Rev. B **64**, 144406 (2001).
[16] K. Mydeen, P. Sarkar, P. Mandal, A. Murugeswari, C. Q. Jin, and S. Arumugam, Appl. Phys. Lett. **92**, 182510 (2008).
[17] P. Sarkar, S. Arumugam, P. Mandal, A. Murugeswari, R. Thiyagarajan, S. Esaki Muthu, D. Mohan Radheep, C. Ganguli, K. Matsubayshi, and Y. Uwatoko, Phys. Rev. Lett. **103**, 057205 (2009).
[18] Y. Imry and M. Wortis, Phys. Rev. B **19**, 3580 (1979).
[19] B. I. Belevtsev, G. A. Zvyagina, K. R. Zhekov, I. G. Kolobov, E. Yu. Beliayev, A. S. Panfilov, N. N. Galtsov, A. I. Prokhvatilov, and J. Fink-Finowicki, Phys. Rev. B **74**, 054427 (2006).
[20] A. Arrott and J. E. Noakes, Phys. Rev. Lett. **19**, 786 (1967).
[21] B. K. Banerjee, Phys. Lett. **12**, 16 (1964).
[22] V. K. Pecharsky and K. A. Gschneidner, Jr., Phys. Rev. Lett. **78**, 4494 (1997).
[23] H. Wada, S. Matsuo, and A. Mitsuda, Phys. Rev. B **79**, 092407 (2009); P. Kumar, K. G. Suresh, A. K. Nigam, A. Magnus, A. A. Coelho, and S. Gama, *ibid.* **77**, 224427 (2008).
[24] P. Sarkar, P. Mandal, and P. Choudhury, Appl. Phys. Lett. **92**, 182506 (2008).
[25] K. A. Gschneidner, Jr. and V. K. Pecharsky, Annu. Rev. Mater. Sci. **30**, 387 (2000).